Approach of a Fluid Dynamic Model for the Investigation of an Industrial Wet Chemical Process Bath

Mohr Lena[a)], Zimmer Martin

Fraunhofer Institute for Solar Energy Systems ISE, Freiburg, Germany

a)Corresponding author: lena.mohr@ise.fraunhofer.de

Abstract. Simulation of the fluid flow in a basin of a wet chemical batch plant for silicon solar cells gains a deeper understanding of the processes in the basin. Flow simulations trough elements with large scale differences, e.g. perforated plates, leads to long simulation time. Perforated plates are used in pipeline systems for the pressure control, before flowmeters to remove swirls in filtering systems or in wet chemical process baths for the rectification of the flow. In a previous work, it was shown that the simulation of a wet chemical process bath with COMSOL Multiphysics® needs a replacement of the perforated plate by a screen feature to save computational time. The screen feature is a two-dimensional plane which changes the flow, according to the perforated plate without solving all dimensions in detail. The implemented screen function in COMSOL is valid to replace perforated plates in the range of a plate thickness t and hole diameter D $t/D \leq 0.20$. With a parameter variation of the perforated plate in a 2D simulation, an adapted screen function is found, to cover the parameter range of $0.25 < t/D < 4.33$. The adapted screen function of $t/D = 0.50$ was transferred in a 3D model and compared with a simulation of a perforated plate. It was found, that the simulation runs five times faster with the adjusted screen function, by reducing the mesh elements from $1.1 \cdot 10^6$ to $0.1 \cdot 10^6$, whereby the mean of e.g. the volume flow is similar, with $\dot{V} = 15 \pm 7$ l/min for the perforated plate and $\dot{V} = 17 \pm 11$ l/min for the adjusted screen feature. The adjusted screen function saves time in simulations that include perforated plates, in particular when it comes to a comparison of different plates.

INTRODUCTION

Silicon solar cells are produced in a series of different process steps in which wet-chemical etching and rinsing steps have a considerable influence on the quality of the wafers [1]. Etching baths are used for surface structuring or intended etch back. Examples therefore are texturing [2,3], cleaning and conditioning [4] or etch back of the front emitter to improve electrical properties of the solar cell [3,5]. In the bath, the process solution is circulated by a pump, which pumps the solution into a supply pipe, through a perforated plate, along the carrier and over an overflow collar back to the pump (Fig.1 a). The requirements for optimal flow conditions over each individual wafer surface are very high, since different etching rates can result from an uneven flow [6]. By the use of computer-controlled flow simulations, the flow in an existing bath from the supply pipe to the overflow collar was simulated (Fig. 1 b) [7], with the aim of gaining a deeper understanding of the processes in the bath and optimizing the geometry for the future. Since the bath contains several disturbances with partial high scale differences, which leads to long simulation times and increased simulation costs, a simplification had to be found. For example the radius of the holes in the perforated plate (3 mm) and the wafers, with a thickness of 180 µm, in the carrier show large scale differences compared to the entire basin (Fig. 1 a) [7]. These condition make the simulation complicate, even if only a quarter of the basin, divided by the symmetry axe is used. In Mohr (2017) it was shown, that the replacement of the perforated plate by COMSOLs integrated screen feature did not match. The velocity was underestimated as well as the pressure, although the simulation cope could be reduced from $4.5 \cdot 10^5$ to $3.5 \cdot 10^4$ mesh elements [7]. In this study a parameter variation of the perforated plate in 2D is done and an adjusted screen function is introduced, which does not underestimate the pressure and velocity. One function is transferred in a 3D model and compared with a simulation of a perforated plate. The adjusted screen function reduces computing time in later variations of geometry, or parameter, such as temperature, flow rate, number of wafers or changes in geometry.

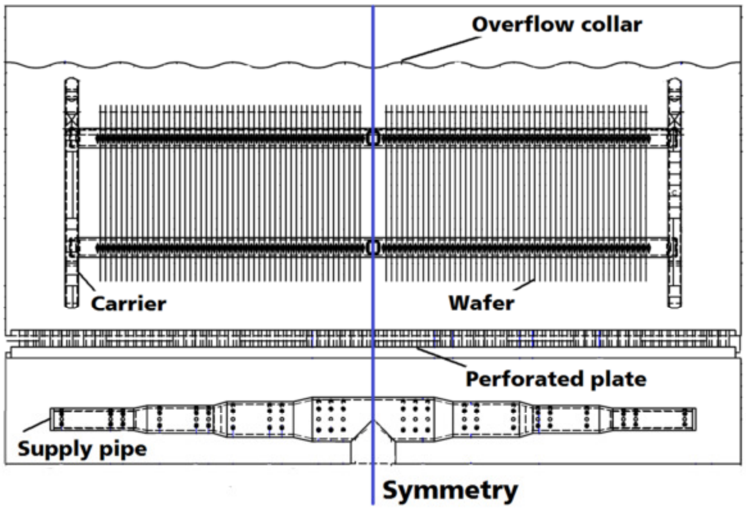

(a)

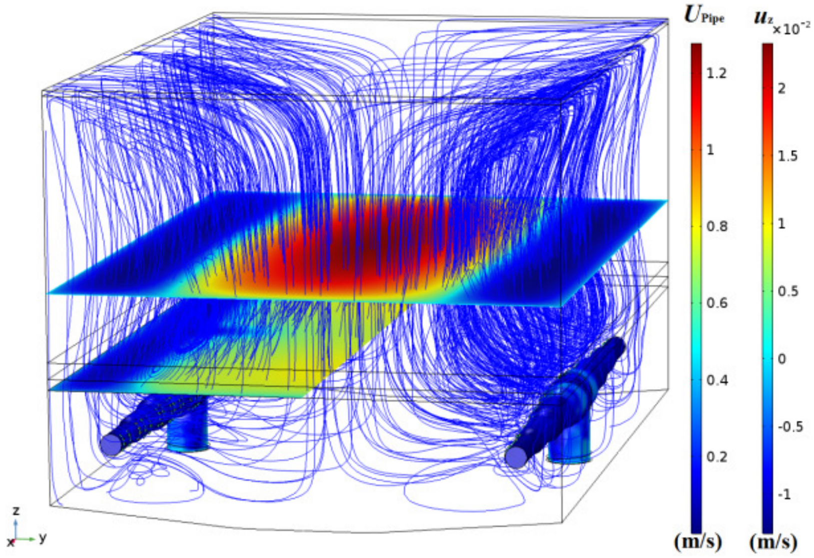

(b)

FIGURE 1. Side view of the basin, with overflow collar, carrier, wafer, perforated plate, supply pipe and the symmetry axis. Simulation results of the velocity magnitude in the pipe U_{pipe} in m/s, and the velocity in z-direction u_z in m/s at a lower and upper work plane and the streamlines. Taken from [7].

APPROACH

The screen feature is implemented in COMSOL and models for instance perforated plates as thin permeable barriers, includes common correlations for resistance and refraction coefficients [8,9]. It simplifies the calculation of a barrier, in this case a perforated plate, by assuming that the width of the barrier is small compared to the resolved length scales of the flow field and thus it can be modeled as an edge in 2D or surface in 3D [8]. The general influence of a perforated plate on the flow field is a loss of the normal momentum component, a change of direction, related to a suppression of the tangential velocity component, a weakening of the kinetic turbulence energy and the maintenance of the turbulence length scale [9]. The following conditions along the screen feature are deposited in COMSOL [10], whereby – is before the feature and + after the feature.

$$[\rho \mathrm{u}\cdot \mathrm{n}]_{-}^{+}=0 \tag{1}$$

$$\left[\rho(\mathrm{u}\cdot\mathrm{n})^2+\mathrm{p}-\mathrm{n}^{\mathrm{T}}\left\{(\mu+\mu_{\mathrm{T}})\left(\nabla\mathrm{u}+(\nabla\mathrm{u})^{\mathrm{T}}-\frac{2}{3}(\nabla\cdot\mathrm{u})\mathrm{I}\right)-\frac{2}{3}\rho k\mathrm{I}\right\}\mathrm{n}\right]_{-}^{+}=-\frac{\mathrm{K}}{2}\rho_{-}(\mathrm{u}_{-}\cdot\mathrm{n})^2 \tag{2}$$

$$\mathrm{n}\times\mathrm{u}_{+}=\eta(\mathrm{n}\times\mathrm{u}_{-}) \tag{3}$$

$$\mathrm{k}_{+}=\eta^2 k_{-} \tag{4}$$

and dependent of the turbulence model

$$\varepsilon_{+}=\eta^3\varepsilon_{-}\ \text{or}\ \omega_{+}=\eta\omega_{-} \tag{5}$$

With the usual flow variables, such as the density ρ, the velocity field u, the normal vector n, the pressure p, the dynamic viscosity μ, the eddy viscosity μ_T, the temperature T, the identity matrix I and the turbulent flow variables, the turbulent kinetic energy k, the dissipation rate ε, the characteristic frequency ω. Equation (1) is the screen boundary condition, Eq. (2) the Navier-Stokes equation on the screen edge/surface, Eq. (4) the damping of the kinetic energy, which depends on the suppression of the tangential velocity Eq. (3). Equation (5) depends on the turbulence model used. Above all, the screen function is adjusted by the pressure loss coefficient K, the refraction coefficient η, the solidity σ (σ = closed area / total area) or the porosity β (β = permeable area / total area = 1 - σ). In particular, K, which is described by default in COMSOL via Equation (6), is of great interest, since the flow can be adapted to a perforated plate via this connection.

$$\mathrm{K}=\mathrm{A}\left((1-\sigma)^{-2}-1\right)^{B} \tag{6}$$

When used in Comsol, only K and η can be adjusted since σ or respectively β, are given by the geometry. The refraction coefficient η, which is between 0 and 1, directs the flow directly after the edge, or surface in one direction. And according to Eq. (4) and Eq. (5) the refraction coefficient influences the turbulence behavior. In Roach [9] and Wiles et al. [11] K was determined in Eq. (6) as a function of the constants A = 0.94 and B = 1.28. Equation (6) is valid for the ratio of the plate thickness t to the hole diameter D in the range of $t/D \leq 0.2$, and for a solidity $0.72 < \sigma < 0.90$. The options provided by the plant manufacturer for optimizing the perforated plate are between $0.35 < \sigma < 0.88$ and the ratio $0.25 < t/D < 4.33$. This is why COMSOL's default equation cannot be used in this parameter study. For this reason, several equations for describing the pressure loss due to perforated plates have been researched. Malavasi et al. [12] investigated various pressure loss relationships due to perforated plates:

- The standard screen function K, already used by COMSOL [10], with an adjusted A, see Eq. (7), but as already mentioned, only a subset of optimization possibilities is covered.
- Idelchick [13] and Huang et al. [14], which additional includes the friction value λ, valid in the range $t/D > 0.015$. Whereby [13] uses the Reynolds number $Re_h=(V_h \cdot D)/\upsilon$ with the hole diameter D and the mean velocity V_h and [14] the pipe Reynolds number $Re_p=(V_p \cdot D_p)/\upsilon$, with the pipe velocity V_p and the pipe diameter D_p.
- Wiles et al. [11] postulated empirical equations depending on the solidity, with different coefficients, which are provided in graphical form. With the $Re=(V_h \cdot D_p)/\upsilon$.
- Others are Zhao et al.[15] and Holt et al. [16], which do not consider a plate thickness [15] or the formula refers to a plate thickness of 2 mm [16]. Whereby [15] uses $Re_p=(V_p \cdot D_p)/\upsilon$ and [16] $Re=(V_h \cdot D_p)/\upsilon$.

Pinker and Herbert [17] propose an adapted constant A for $t/D \geq 0.2$

$$\mathrm{A}=0.94/\left(1+3\left(\frac{t}{D}\right)^4\right) \tag{7}$$

,valid for $0 < t/D < 0.8$ and $0.05 < \sigma < 0.95$

The above mentioned diverse relationships complicate the actual reason of replacing the standard function K by using aditional factors [13], which are only graphically available [11] or do not include the thickness of the perforated plate [15,16]. Equation (6) must be adjusted according to Pinker and Herbert [17], since in Eq. (7), in contrast to Eq. (6), the ratio t/D is taken into account, but not for the entire optimization range. That is why an adjusted screen function K_a must be found, to describe the perforated plate for different t/D and σ ranges.

EXPERIMENTAL SET-UP

2D Model

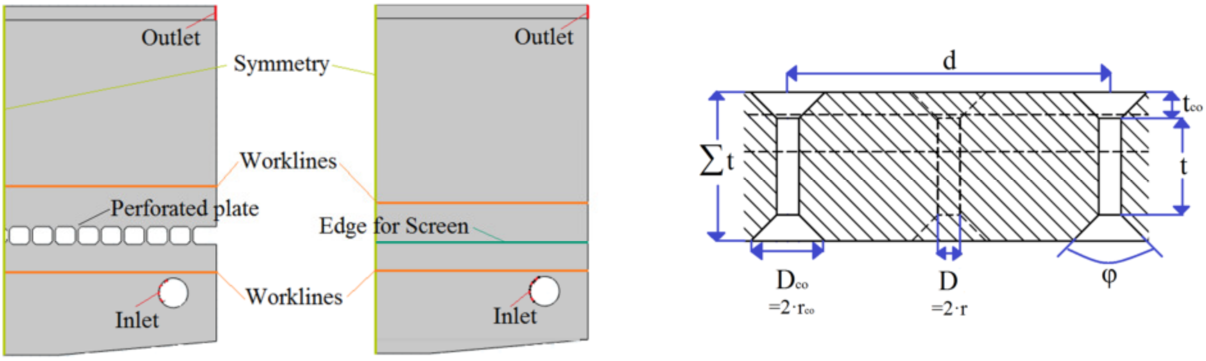

(a) (b) (c)

FIGURE 2. 2D model with work lines, 30 mm below and 44 mm above the perforated plate/edge, inlets at the supply pipe, and perforated plate (a) in the ratio t/D = 1.3 and σ = 0.35, respectively edge for use of Eq. (6) (b). Scheme of the perforated plate with distance between the holes d, sum of material thickness ∑t, material thickness conical part t_{co}, material thickness cylindrical part t, diameter of the conical D_{co} and cylindrical part D (c). The hole angle was kept constant in the variation.

The simulations were done with water as initial material during a temperature of 293.15 K. Due to the symmetry, Fig. 2 shows half of the cross section of the bath in 2D, with a perforated plate and the edge on which, according to Eq. (6) the flow can be changed; including the inlets of the supply pipe, two work lines for the evaluation of the pressure loss coefficient, 44 mm above and 30 mm below the perforated plate/edge and the outlets on the upper right of the bath. Detailed investigations of the flow below and above the perforated plate, under parameterization of the plate geometry (Fig. 2 c), were simulated and compared with the results of an adjusted screen function. Figure 2 c shows the parameters which ca be varied, with distance of the holes from each other d, sum of material thickness ∑t, material thickness of the conical part t_{co}, material thickness of the cylindrical part t_{cy}, diameter of the conical D_{co} and cylindrical part D. In a first simulation, the perforated plate was parameterized, whereby the perforated plate geometry corresponded to the production possibilities of the plant manufacturer. A Design of Experiments (DOE) was prepared as shown in Fig. 3.

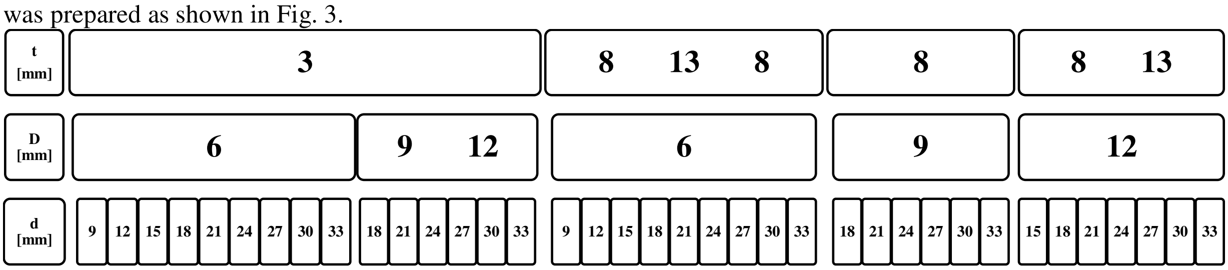

FIGURE 3. Design of Experiments (DoE) varied in material thickness of the cylindrical part t, diameter of the cylindrical part D and the distance between the holes d.

The DoE consisted of 68 different parameter combinations, in thickness t, diameter of the cylindrical part D and distance between the holes d. The purpose of the plate is to direct the flow in the normal direction, so that the results of the parameter study led to a correlation between the varied parameters and the observed physical values: velocity magnitude U in m/s and pressure p in Pa. The observed correlation led to a function K_a, in which the parameter A_a is adjusted and replaced the COMSOL integrated function K. σ was calculated according to Eq. (8), with data from Fig. 3, whereby w in mm is the width of the bath, d the distance between the holes in mm and N the numbers of holes in the perforated plate.

$$\sigma = \frac{w - (N \cdot D)}{w} \quad \text{with } N = \frac{w}{d + 1\,\text{mm}} \tag{8}$$

3D Model

The 2D results were transferred to a 3D model, so that the edge on which the screen function is applied corresponds to a surface. To save computational time, a part of the bath is simulated with a perforated plate and compared to a model with a surface on which the adjusted function is applied (Fig. 3), with a volume flow at the inlets of the supply pipe of 16.7 l/min.

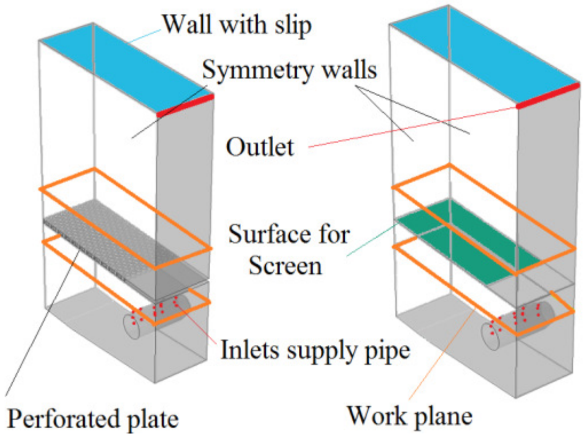

FIGURE 4. Part of the bath with w = 41mm with work planes, 30 mm below and 44 mm above the perforated plate/surface and inlets of the supply pipe, as well as the outlet, perforated plate in the ratio t/D = 0.5 and σ = 0.6657 (left) and surface for using the screen function, at A = 0.77, σ = 0.6657 and η = 1 (right).

In a 3D Model σ is calculated via.

$$\sigma = \frac{\left(w \cdot (1 - 62.62\,\text{mm}) - \left(N \cdot \pi \cdot \left(\frac{D}{2}\right)^2\right)\right)}{w \cdot (1 - 62.62\,\text{mm})} \quad \text{with } N_y = \left(\frac{1 - 61.62\,\text{mm}}{d_y + (D)}\right) \text{ and } N_x = \left(\frac{w}{d_x + (D)}\right) \tag{9}$$

The perforated plate was set up with the parameters σ = 0.6657 and t/D = 0.50 and compared with the adjusted screen function with A = 0.77, σ = 0.6657 and η = 1. Since the feasibility to transfer the adapted function to a 3D model is observed, the simulation was done on a rough mesh.

RESULTS AND DISCUSSION

The evaluation took place on the above mentioned work lines and planes. The pressure loss coefficient between this work lines or respectively planes was calculated according to the Euler number:

$$Eu = \frac{p_U - p_D}{\frac{1}{2}\rho U^2} \tag{10}$$

Where p_U and p_D describe the upstream and downstream pressure. U is the mean velocity magnitude before the flow obstruction [13]. The position of U and D are defined in various ways due to the many existing standards [12]. In particular, in pipe flow, U requires ten times the pipe diameter upstream and D fifteen times the pipe diameter downstream[18]. In this work, the two positions were held 30 mm below and 44 mm above the perforated plate during parameter variation.

2D Model

The pressure below and above the perforated plate were given on the work lines. U = 0.202 m/s was previously determined by a simulation without any flow obstruction. According to Eq. (10), Eu was calculated. In order to compare the perforated plate with the original screen function, the pressure loss was plotted as the Euler number against the term $((1-\sigma)^{-2}-1)$ of Eq. (6), in which the solidity is included.

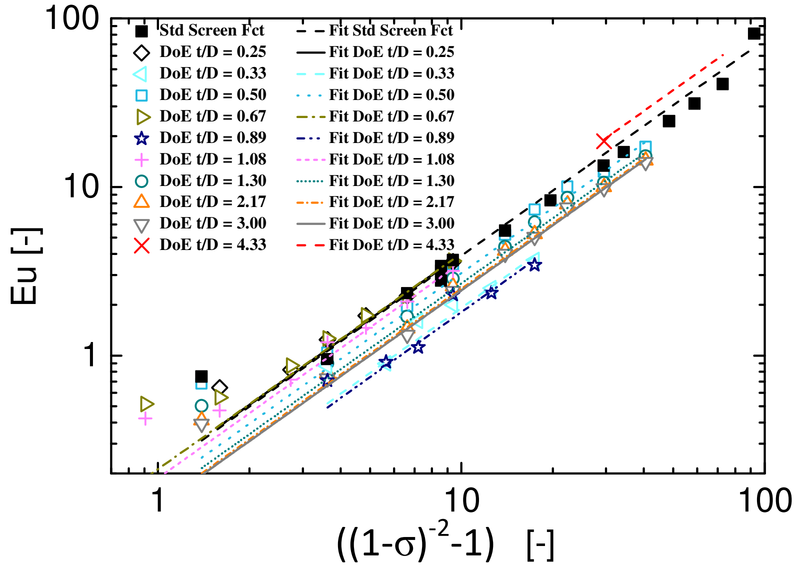

FIGURE 5: Euler number Eu of the standard screen function on the edge (closed symbols) and the results of the DoE simulation of the perforated pate (open symbols), for different ratios of t/D, against $((1-\sigma)^{-2}-1)$. With fits, according to Table 1.

Eu rises with increasing solidity for the standard screen function in closed-symbols, and the DoE for the perforated plate in open symbols (Fig. 5). During the simulation the standard screen function did not converge for solidities, between $0.9 < ((1-\sigma)^{-2}-1) < 8$ three of nine points converge. The standard screen function does not take t/D into account. The parameter A of the standard screen function in Eq. (6) must be adjusted, according to Pinker and Herbert [17], to include the ratio t/D. With a fit, according to the fit function (Table 1), the parameter C is given for each curve, seen in Table 1 and plotted in Fig. 5. The fit of the curves was done according to Eq. (6), whereby B kept constant to B = 1.28. If Eq (6) with A = 0.94 becomes C = 0.200 than A has to be adjusted, according to $A_a = 4.7 \cdot C$, to shift the curve for a given t/D. For example for t/D = 0.5 with C = 0.162 A has to be $A_{a,\,0.5} = 0.76$.

TABLE 1: Fitted parameter of C, according to the fit function with standard Error, reduced Chi-Squared x^2, corrected R-squared R^2 for the standard screen function (Std Screen Fct), and the adjusted parameter A_a at different t/D ratios.

Fitted parameter of Fig. 5					
t/D **Correspond to**	**Fit function: $Eu = C\cdot((1-\sigma)^{-2}-1)^{1.28}$** **C**	**Std Error**	**x^2**	**R^2**	**Adjusted parameter** **A_a**
Std. Screen Fct	0.200	0.0102	25.069	0.947	
0.25	0.210	0.0071	0.027	0.978	0.99
0.33	0.100	0.0050	0.069	0.940	0.47
0.50	0.162	0.0052	0.675	0.979	0.76
0.67	0.212	0.0082	0.036	0.972	1
0.89	0.096	0.0062	0.104	0.908	0.45
1.08	0.187	0.0069	0.104	0.974	0.88
1.30	0.141	0.0038	0.026	0.986	0.66
2.17	0.131	0.0027	0.354	0.992	0.62
3.00	0.128	0.0023	0.182	0.994	0.60
4.33	0.251	0.0119	0.130	0.969	1.18
Fitted parameter of Fig. 6					
t/D **A_a**					
0.33 0.47	0.108	0.0019	0.013	0.993	
0.50 0.76	0.146	0.0034	0.298	0.987	
2.17 0.62	0.121	0.0035	0.305	0.981	

This assumption was verified by using the adjusted function with the adjusted parameters A_a according to Table 1 (underlined) for a simulation. The results of three sets (t/D = 0.33, 0.50 and 2.17) are shown in FIG. 6. The DoE results are shown in open symbols, the half-filled symbols are the results with the adjusted parameter A_a. It is demonstrated, that the adjusted function replaces the perforated plate instead of the standard screen function, which is shown in the full-filled symbols. Also, the adjusted functions converge for lower solidity ranges and take the ratio t/D into account.

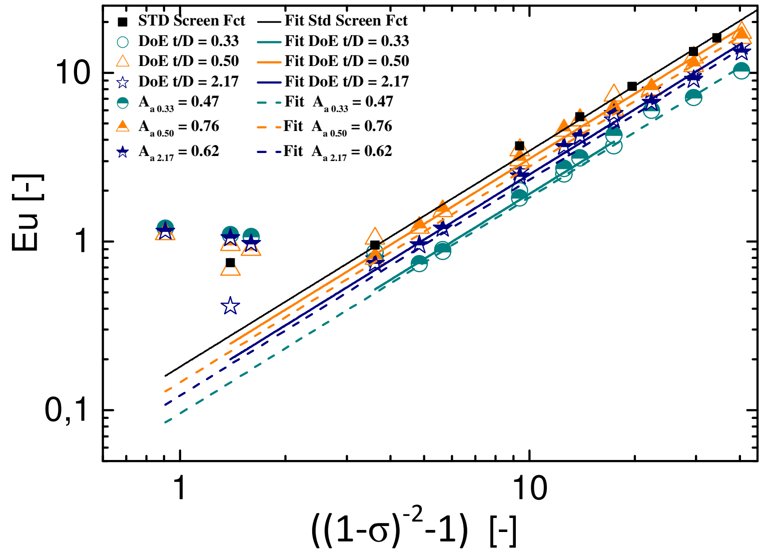

FIGURE 6: Euler number Eu of the standard screen function (closed symbols), three DoE simulations with t/D = 0.33, 0.50, and 2.17 (open symbols) and the results with the adjusted function (half-filled symbols), including the adjusted parameter A_a against $((1-\sigma)^{-2}-1)$. With fits, according to Eq. (6) and Table 1

3D Model

The results obtained in 2D were transferred to a 3D Model, this was done for a perforated plate at a ratio of t/D = 0.5 with a solidity of σ = 0.6657 and compared to an adjusted screen function with A_a = 0.76 and σ = 0.6657. The mean values of the pressure p, velocity magnitude U, the volume flow $\dot{V}$ and the standard deviation on the upper work plane for the perforated plate (n=348) and the adjusted and standard screen function (n=261) are shown in Table 2, as well as the number of mesh elements M and computational time of the 3D model.

TABLE 2: Mean±standard deviation of the pressure p, velocity magnitude U, the volume flow $\dot{V}$ on the upper work plane. As well as the number of mesh elements N and the computational time of the 3D model.

Simulation of	p_D [Pa]	U [m/s]	$\dot{V}$ [l/min]	M [-]	Time [min]
Perforated plate	122±0.05	0.0133±0.006	15.0±6.8	$1.1\cdot10^6$	7523
Adjusted screen function	134±0.06	0.0115±0.009	17.0±11.0	$0.1\cdot10^6$	1429
Standard screen function	133±0.11	0.0107±0.004	12.0±4.8	$0.1\cdot10^6$	840

The theoretical volume flow on the inlets of the supply pipe is 16.7 l/min, the flow on the upper work plane of the standard screen function is 12.0 l/min which is about 5 l/min higher then the volume flow of the adjusted screen function with 0.3 l/min.

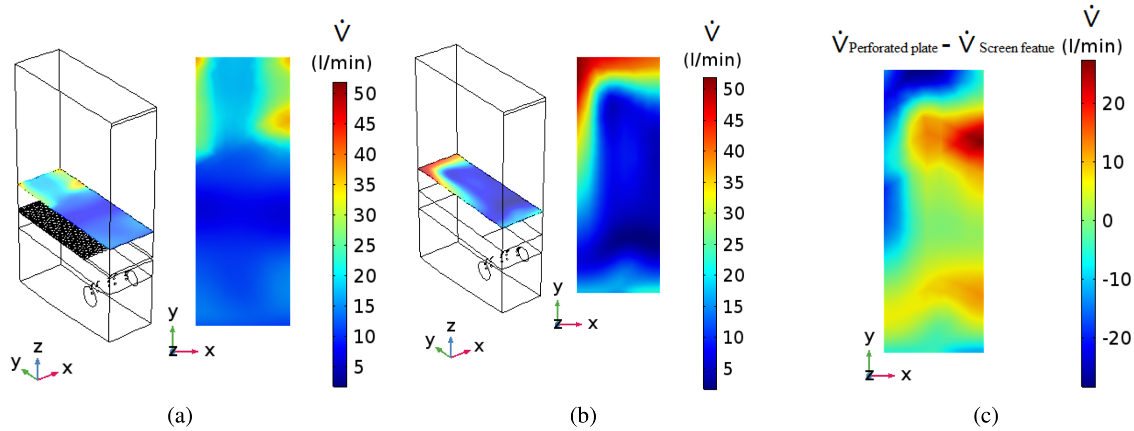

FIGURE 7: Volume flow V̇ in l/min on the work plane for the perforated plate (a) and the adjusted screen feature (b). And the difference between the two solutions on the upper work plane (c).

The volume flow V̇ is plotted for the model with the perforated plate (Fig 7 a) and the screen feature (Fig. 7 b) on the upper work plane. In the upper part of the work plane differences of up to -20 l/min are simulated (Fig 7 c), where the difference of the volume flow of the perforated plate and the adjusted screen function is calculated. Strong differences with up to 20 l/min can be seen on the upper right part of the work plane. The sharper edges in this part of the figure are mesh artifacts and result from the rough mesh of the geometry. The results show, that there is a negligible small difference of 2 l/min between the perforated plate and the adjusted screen function in the mean values on the work plane (Table 2).

For a pointwise precise flow in the basin, the screen function should not be used, but it saves a lot of time for optimizing simulations, for example to observe the flow by changing the position of the inlet pipe, by parameterize the inflow velocity or temperature. It should be noted that through the adapted screen feature in addition to the computational time listed in Table 2, more time can be saved in the building of the geometry. A model with all its resolved scales, such as the perforated plate, takes much more time in the construction, compared to an insertion of a surface. Especially if it comes to the construction of the entire basin, which is in size more than three times of the part shown in FIG. 4. And the saving of computing time makes itself noticeable in a subsequent parameterization, e.g. the volume inflow or the adaptation of the position of the inflow pipe.

PRACTICAL APPLICATION

With the aim of simulating holistic chemical etching processes for photovoltaics, the perforated plate shows itself as an example of the recurring application that the simulation of flows through elements with very large size differences is very complex. The structured approach from the 2D model and the transfer in a 3D model can be applied in various process simulations in which perforated plates are used: (a) pipeline systems, to reduce nonuniformities or control the pressure (b) before flowmeters to remove swirls (c) as well as in filtering systems. In the photovoltaic industry, perforated plates are used in wet chemical batch systems (d), but also in hand wet benches (e). Especially in the batch plants, the perforated plates were installed; neither the mode of action nor the benefit has been systematically investigated so far. For these systems the screen function can be used, for the considered range of plate thickness t and hole diameter D $0.25 < t/D < 4.33$. Although the function should not be used for the exact description of the flow pattern, it is possible to simulate the pressure conditions realistically in a shorter computing time. Especially, when planning new plants and processes with circulation through perforated plates, the function saves time, as it gives an overview of the need for perforated plates and when it comes to a comparison of different plates.

CONCLUSION

The COMSOL's standard equation K did not converge for all solidities σ and has not the opportunity to include t/D. An adjusted function $K_a = A_a \cdot ((1-\sigma)^{-2}-1)^{1.28}$ was found whereby different parameters A_a correspond to different t/D ratios. This assumption was verified, by using this equation and compares it with the real perforated plate parameters. It was demonstrated, that the adjusted screen function replace the standard screen function and takes the ratio t/D into account. The results obtained in 2D were transferred to a 3D model, this was done for a perforated plate at a ratio of t/D = 0.5 with a solidity of σ = 0.6657 and compared to an adjusted screen function with A_a = 0.76 and σ = 0.6657. The 3D simulation with the adjusted screen function runs five times faster than the perforated plate, whereby the mean values of e.g. the volume flow are similar, with $\dot{V} = 15 \pm 7$ l/min for the perforated plate and $\dot{V} = 17 \pm 11$ l/min for the screen feature. It is assumed, that for a pointwise precise flow in the basin, the screen function cannot be used, but it should be used for optimizing simulations, e.g. the observation of the flow by changing the position of the inlet pipe, during parameterization the inflow velocity or temperature. For Systems including a perforated plate, e.g. pipeline or filtering systems, the screen function can be used, to simulate within a shorter time the realistic pressure conditions for the range of plate thickness t and hole diameter D $0.25 < t/D < 4.33$.

ACKNOWLEDGEMENTS

This work was funded by the German Federal Ministry for Economic Affairs and Energy „CHEOPS“ (0324056B).

REFERENCES

1. A. Goetzberger, B. Voß, and J. Knobloch, *Sonnenenergie: Photovoltaik. Physik und Technologie der Solarzelle : Mit 2 Tabellen* (Stuttgart: Teubner, Stuttgart, 1994).
2. E. Vazsonyi, K. de Clercq, R. Einhaus, E. van Kerschaver, K. Said, J. Poortmans, J. Szlufcik, and J. Nijs, Solar Energy Materials and Solar Cells **57** (1999).
3. A. Lachowicz, K. Ramspeck, P. Roth, M. Manole, H. Blanke, W. Hefner, E. Brouwer, B. Schum, and A. Metz (2012).
4. W. Kern, ed., *Handbook of semiconductor wafer cleaning technology* (Park Ridge, N.J.: Noyes Publications, Park Ridge, N.J, 1993).
5. A. Moldovan, K. Birmann, J. Rentsch, M. Zimmer, T. Gitte, and J. Fittkau, Diffusion and Defect Data Pt.B: Solid State Phenomena **195** (2013).
6. A. Moldovan, *Ozonbasierte Reinigungs- und Konditionierungsverfahren für die Herstellung hocheffizienter Silizium Solarzellen* (Fraunhofer Verlag, Stuttgart, 2016).
7. L. Mohr, M. Zimmer, A. Moldovan, M. Menschick, B. Mandlmeier, and C. Müller, COMSOL Conference, Rotterdam, Netherlands (2017).
8. COMSOL 5.2a, ed., *COMSOL Multiphysics 5.2*, COMSOL Reference Manual (2016).
9. P. E. Roach, International Journal of Heat and Fluid Flow **8** (1987).
10. COMSOL 5.2a, ed., *COMSOL Multiphysics 5.2a*, CFD Model User Guide (2016).
11. W. F. Wiles, E. C. Firman, B. H. Fisher, G. Hobson, J. M. Ilsley, T. V. Lawson, J. Pederson, and C. Scruton, Engineering Sciences Data Item (1972).
12. S. Malavasi, G. Messa, U. Fratino, and A. Pagano, Flow Measurement and Instrumentation **28** (2012).
13. I. E. Idelchick, 1986 (1986).
14. S. Huang, T. Ma, D. Wang, and Z. Lin, Experimental Thermal and Fluid Science (2012).
15. T. Zhao, J. Zhang, and L. Ma, Journal of Mechanical Science and Technology **25** (2011).
16. G. J. Holt, D. Maynes, and J. Blotter, *Cavitation at sharp edge multi-hole baffle plates* **6** (2011).
17. R. A. Pinker and M. V. Herbert, Journal of Mechanical Engineering Science **9**, 11 (1967).
18. H.-f. Liu, H. Tian, H. Chen, T. Jin, and K. Tang, J. Zhejiang Univ. Sci. A **17** (2016).